



IUTAM Symposium on Multiphase flows with phase change: challenges and opportunities,  
Hyderabad, India (December 08 – December 11, 2014)

## Coupled DEM-CFD model to predict the tumbling mill dynamics

K. Mayank<sup>a</sup>, M. Malahe<sup>b</sup>, I. Govender<sup>b</sup>, N. Mangadoddy<sup>a</sup>

<sup>a</sup>IIT Hyderabad, Yeddumailaram, Medak 502205, India

<sup>b</sup>University of Cape Town, Rondebosch 7701, South Africa

---

### Abstract

The charge motion in a tumbling mill has been mostly described by empirical, mechanistic and computational models. The computational model presented in this work is a three phase approach for the tumbling mill that combines a particle description for the solids modelled by the Discrete Element Method, and the continuum description for the fluid by CFD approach. In the present work a phase coupled approach is developed using C++ subroutines to model the charge and slurry dynamics inside a tumbling mill by mapping the particles on the CFD mesh and resolving the particle volume and velocities on per cell basis. The coupled DEM-CFD approach is implemented and the effect of drag force on the slurry by the particle motion. The set of coupled simulation were run varying the slurry rheology and results were validated with equivalent PEPT experiment of lab scale mills and a very good agreement is found in some cases. The Beeststra drag correlation was used to calculate the drag force between the fluid and the particles. The free surface profile of the charge as well as the slurry is calculated as well as the axial center of mass profile of the mill.

© 2015 The Authors. Published by Elsevier B.V. This is an open access article under the CC BY-NC-ND license (<http://creativecommons.org/licenses/by-nc-nd/4.0/>).

Peer-review under responsibility of Indian Institute of Technology, Hyderabad.

**Keywords:** DEM , CFD , Coupling DEM-CFD , Tumbling mills

---

### 1. Introduction

Grinding is an important unit operation used in the chemical or mineral industry for size reduction. In mineral processing industries the tumbling mill are extensively used machines for producing fine particle size reduction through attrition and compressive forces at the grain size level. The Autogenous and Semi Autogenous mills in particular causes self grinding of ore as the feed to these mills are water and large ore particles in the feed collide with other particles due to the rotating action of the mill and breaks down into smaller sized particles due to the compressive forces and the frictional force between the particles cause the production of much finer size particles by a nibbling action. The water that is in feed forms slurry with the finer size particles and facilitates the discharge of the grinded ore particles out of the mill through a grate at the discharge end that prevents the ungrinded particles to pass through.

---

\* Kumar Mayank. Tel.: +919960612179

E-mail address: [ch12m1006@iith.ac.in](mailto:ch12m1006@iith.ac.in)

Though extensively used in mineral industries these mills are highly energy inefficient. According to a survey presented in<sup>1</sup> for copper production milling accounts for roughly 60 percent of the total energy input. The total grinding energy can be segregated into energy consumed in elastic deformations, plastic deformations, lattice rearrangement and new surface energy. External to the particle friction between particles and grinding media as well as other particles, sound energy, kinetic energy of products and deformation of the grinding media also constitute a significant amount of input energy. Out of all these the amount of energy needed for fracture i.e. the new surface energy is only a small fraction around 1-5 percent<sup>2</sup>.

The slurry formed by the mixing of the feed water and the fine ore particles are very significant for the material transport to the grinding zone and subjecting the mineral ores for grinding action. Followed by the transport of the fine ore through the discharge. Any parameter affecting these processes will affect the grinding efficiency. The probability of overall breakage is the product of the probability of capture in the grinding zone and the probability of breakage upon capture<sup>3</sup>. Therefore effective knowledge of slurry dynamics can be very useful for modeling the charge motion of these mills and for the design of mills with increased probability of particles being captured in the grinding zone. Slurry pooling is also an important issue in the mills especially at the toe region where there should be an optimum amount of slurry, a higher amount of slurry caused damping of the impact force on the particles and too low slurry may cause unnecessary wear of the mill liner. Visual representation of charge and slurry motion can be used for efficient lifter design such that maximum cascading of the particles take place and the cataracting particles fall near the toe region of the mill such that both the impact as well as frictional force are effectively used for breakage of particles.

Discrete element modeling is a well established method to predict the charge motion in ball mills as presented by Mishra<sup>4</sup> and Cleary<sup>5</sup> where the each particle is tracked individually and forces are calculated using the soft sphere approach. Although extensively used to model the charge motion the DEM model fails to account for the effect of slurry on the solids. To account for the slurry effects coupled models are used. To account for particle fluid interaction previously DEM has been coupled with SPH where the shear force between the phases are induced artificially using permeability model as the continuous phase is treated as discrete particles and tracked individually, this method is computationally very expensive if the domain is very large then tracking each particle will increase the time required for simulation. The work presented in this study is to prepare a computational model that can accurately predict the complex multiphase dynamics of charge, air and slurry inside the mill using a coupled model between computational fluid dynamics and discrete element method.

### Nomenclature

$m$	mass of particle
$F_{ii}$	Contact force
$v$	Velocity of particle
$u_f$	Velocity of fluid
$g$	Acceleration due to gravity
$q$	Damping coefficient
$k$	Spring coefficient
$x$	Deformation of the particle
$\rho_i$	Density of phase i
$\mu$	Dynamic viscosity
$v$	Velocity of particle
$\phi$	Solidicity
$F$	Non-dimensional drag term
$Re$	Reynolds number
$\epsilon_i$	Volume occupied by phase i

## 2. Literature Review

The high energy requirement and low efficiency of the milling equipments has caused much of modern day comminution research being focussed on accurately predicting the charge and slurry dynamics inside the tumbling mills. Earliest attempt to model the charge motion inside the ball mill was done by Rajamani and Mishra<sup>4</sup> in which a computer code was developed using the 2 dimensional discrete element method to model the ball motion inside the mill, validating their model by comparing the simulated values of torque with experimental results. They further extended their study for 3D mills<sup>6</sup> validating their predicted charge motion with experimental video captured by high speed camera. Since DEM modeling requires only material properties as inputs the scale up for simulating industrial scale autogeneous mill was followed in their future work<sup>7</sup>. Alkac and Rajamani<sup>8</sup> used a pure CFD approach to model the slurry flow in pulp lifter channels to study the discharge rate and free surface profile at the discharge end predicting the actual throughput of the mill. The coupling algorithm used by Tsuji underwent several improvements with respect to handling viscous fluid flows<sup>9</sup>, incorporating turbulence modeling for the fluid flow<sup>10</sup>, effective parallelization over several GPU for faster computation<sup>11</sup>. Cleary<sup>12</sup> was the first to present a SPH-DEM coupled model to study the slurry dynamics inside the mill modeling the solid particles by DEM and the slurry by SPH, the drag force was implemented using the Kozeny-Carmen permeability model for slurry flow past the porous solid medium was used for interaction between slurry and the solid phase. Morrison and Cleary<sup>13</sup> presented the Virtual Comminution Machine simulation code to model the breakage and slurry transport inside the mill. Combining CFD and DEM Jayasundara et.al.<sup>14,15</sup> studied the effects of slurry properties on the charge flow and power draw in a stirred mill concluding that slurry density and viscosity have profound effect on the charge motion. The present work is similar to the coupling work done by Jayasundara et.al. the difference in the two coupled models are that this study focussed on the study of the effects of solid motion on the fluid phase to model the free surface profile of the slurry air system.

## 3. Modeling fluid-particle system

### 3.1. Modeling particle motion

The larger sized particles present in the tumbling mill are modeled using the discrete element method where the governing equation for the particle flow is the Newton's second law of motion where the force is calculated based on deformation of the particles using hertzian model which is

$$m \frac{dv}{dt} = F_{ii} + m_i g \quad (1)$$

$F_{ii}$  is the contact force which can be calculated using the non-linear hertzian model.

$$F_{ii} = -qx^{0.25} \frac{dx}{dt} - kx^{1.5} \quad (2)$$

### 3.2. Modeling fluid motion

The governing equation for the multiphase flow of incompressible fluid is the equation of continuity and the Navier Stokes Equation

$$\frac{\partial(\epsilon_f \rho_f)}{\partial t} + \nabla \cdot (\epsilon_f \rho_f u_f) = 0 \quad (3)$$

$$\frac{\partial(\epsilon_f \rho_f u_f)}{\partial t} + \nabla \cdot (\epsilon_f \rho_f u_f u_f) = -\nabla p + \nabla \cdot \tau_f + \epsilon_f \rho_f g + F_{fp} \quad (4)$$

Where  $\epsilon_f$  is the fluid volume fraction,  $\rho_f$  is the fluid density,  $\tau_f$  is the viscous stress of the fluid, for a Newtonian fluid we can replace  $\nabla \tau_f = \mu \nabla^2 u_f$ ,  $p$  is the fluid pressure,  $u_f$  is the fluid velocity, the fluid particle interaction force is denoted by  $F_{fp}$ . As both phases are incompressible, we have the mass conservation equation as:

$$\nabla \cdot (\epsilon_f u_f + \epsilon_s u_s) = 0 \quad (5)$$

using equation (3.10), (3.11) and the relationship between  $\tau_f$  and  $v_f$  for Newtonian fluids in equation (3.9) we have:

$$\frac{\partial(\epsilon_f \rho_f u_f)}{\partial t} + \nabla \cdot (\epsilon_f \rho_f u_f u_f) = -\epsilon_f \nabla p + \epsilon_f \mu \nabla^2 u_f + \epsilon_f \sum_{i=1}^{c_n} \frac{f_{di}}{V_c} + \epsilon_f \rho_f g \quad (6)$$

In the above equation  $\epsilon_f$  is obtained from the relation:

$$\epsilon_f + \epsilon_s = 1 \quad (7)$$

To account for the effect of the drag force from the solids on the fluid we need from the DEM simulations the solid fraction  $\epsilon_s$  as well as the solid field velocity  $u_s$ . The calculation of the drag force is done by using Beetstra drag model<sup>16</sup> in the current work. The non dimensional drag term using Beetstra correlation is given by equation 8.

$$F(\phi, Re) = \frac{10\phi}{1-\phi} + (1-\phi)(1 + 1.5\sqrt{\phi}) + \frac{0.413Re}{24(1-\phi)^3} + \left[ \frac{(1-\phi)^{-1} + 3\phi(1-\phi) + 8.4Re^{-0.343}}{1 + 10^{3\phi}Re^{-(1+4\phi)/2}} \right] \quad (8)$$

### 3.3. Modeling fluid particle interaction

The larger size particles in the mill can be modelled by the discrete element method, the scheme of discrete element method is that it checks for contacts, calculates the force due to the contact, allows finite displacement and rotation due to the force for a given timestep and again checks for contacts at the beginning of the next time step. Whereas the slurry phase can be treated as a continuum and the multi-phase system of air and slurry can be modelled by CFD approach. In the dense particle flow regime drag force is the predominant force that is the cause of momentum exchange between the phases. The implementation of coupling between the phases in the present study is one-way i.e. The forces from the particles affect the fluid but the vice versa is not true. the forces from DEM should be resolved on per cell basis to be added as the source term as given in the governing equation for the fluid(i.e. Eq. 6).

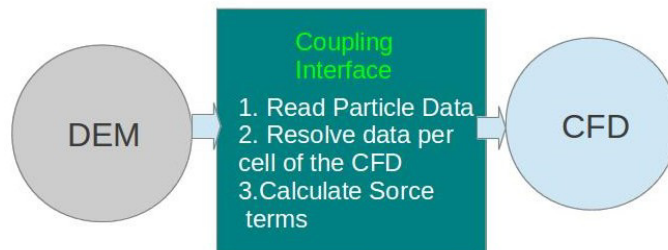


Fig. 1. Coupling Algorithm between DEM and CFD

### 3.4. Coupling Implementation

The correct implementation of the coupling between the discrete and continuous phase the flow variables must be constant over time at least within some statistical bounds. For this to be the case, the force applied by the particles on the fluid should also be steady, which requires the same of the velocity of the particles and the local solidicity. Since the particles are in motion, this will never hold for a given point in the charge, and can only be true over some averaging volume and time. The averaging time interval depends on the relaxation time for the slurry, work by Blakey and James<sup>20</sup> show that laterite slurries having solids concentration less than 9% show almost instantaneous relaxation times under industrial scale shear rates. The slurry phase used in the current work have solid concentration above 20% solids, therefore for the current work the averaging of the forces is done at an interval of 0.0005 sec for slurry with 20% solid concentration and a higher value of averaging time interval is chosen for higher slurry concentration. The volume averaging is done by distributing the mass of the the particle throughout its volume and then averaging the contribution in each of the axis aligned voxels which are associated with the CFD cells. The model parameter used are enlisted in table 3.

$$V_{p,j} = \sum_{i \in \square}^i \frac{V_i N_{i,j}}{N_i}$$

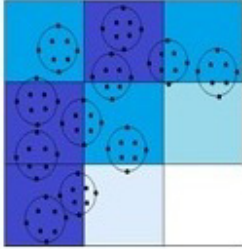
$$v_{avg,j} = \sum_{i \in \square}^i \left( \frac{V_i N_{i,j} v_i}{N_i} \right) / V_{p,j}$$


Fig. 2. Averaging particle volume data over axis aligned voxels

## 4. Numerical Simulation

### 4.1. DEM Model

Initial simulation was done to validate the discrete element method to accurately predict the charge motion inside a tumbling mill. Set of dry DEM simulations were conducted varying and the speed of the mill. The particles were modeled as spherical balls of diameter 5 mm. The material properties of the the particles as well as the mill geometry is given in table 1.

Table 1. Material properties of charge particles and mill shell .

Charge Particles	
Parameter	Value
Density	2200
Shear Modulus	21 GPa
Poisson's ratio	0.22
Mill Shell	
Parameter	Value
Density	2700
Shear Modulus	27 Gpa
Poisson's ratio	0.2

The contact between the particles as well as between particles and mill walls are modelled by non linear hertzian model. The model parameters for contact properties are given in table 2. The Rayleigh time step calculated based

Table 2. Contact properties of charge particles and mill shell .

Particle-Particle Contact	
Parameter	Value
Coefficient of static friction	0.1
Coefficient of rolling friction	0.1
Coefficient of restitution	0.5
Particle-Wall Contact	
Parameter	Value
Coefficient of static friction	0.1
Coefficient of rolling friction	0.1
Coefficient of restitution	0.5

on the above material properties was  $3.37 \times 10^{-6}$  sec. The time step size for the simulation was chosen to be  $1 \times 10^{-6}$  sec. The whole domain was divided into voxels of dimension  $0.15 \times 0.15 \times 0.15$  mm for implementation of the boxing scheme of the contact search, corresponding to 32 voxels in each direction. A total of around 50000 particles were initialized position by filling a cylindrical section centered at origin, having radius 0.125 cm and length of 0.25 cm corresponding to 31.25 % mill loading. Each particle was assigned to zero velocity initially. The commercial code EDEM 2.4 was used to solve the particle motion equations. The non-linear spring dashpot model inbuilt in EDEM was used to model the contact forces.

#### 4.2. Pure CFD Model

The pure CFD Model of the slurry-air system was also simulated to find the free surface profile. Slurry was modeled as incompressible fluid having density  $1148 \text{ kg/m}^3$ . The slurry air multiphase system was modeled using inbuilt volume of fluid model. The turbulence model  $k-\epsilon$  inbuilt in Fluent 13.0 was used to model turbulence. Sliding mesh model was used to incorporate the rotation of the mill. The fluid flow governing equation was discretized using the finite volume method where the pressure velocity coupling was done using SIMPLE algorithm[.]. The volume of fluid model was used to predict the dynamics of the slurry-air multiphase system. The turbulence induced in the slurry-air system due to rotation of the mill was modeled using the  $k-\epsilon$  turbulence model. Commercial CFD solver Fluent 13.0 was used to solve the fluid flow governing equations.

#### 4.3. One way coupled DEM-CFD Model

The coupling in the present study is a one-way in a sense that the DEM simulation was first run completely then the data obtained from the simulations were averaged over time and volume as discussed in subsection 3.3. The averaged data was used to calculate the source terms for each CFD cell for the given time interval. The source term is updated after each time interval over which averaging is done. The slurry phase was modeled as fluid with varying density and viscosity based on the solid concentration present in the slurry. The DEM simulation results run for 5 seconds and the data were averaged over every 0.0005 seconds and the averaged porosity and local velocity data are used to calculate the drag force and the calculated force is updated as source terms in the fluid cells using user defined functions. The models used for multiphase and turbulence modeling is inbuilt, and the addition of the momentum source terms was done using user defined functions. Variable time step size was used to for the simulation fixing the global courant number to 2. . To find out whether the solution obtained has grid dependency the simulation was run using 3 different mesh sizes having 58880, 108214 and 152187 cells respectively. The tangential velocity plot was compared for different mesh size as given in figure 3, It was observed that the solution in case of mesh size having 108214 and 152187 shows slight difference. Therefore in order to reduce the computational cost the mesh size having 108214 cells is used.

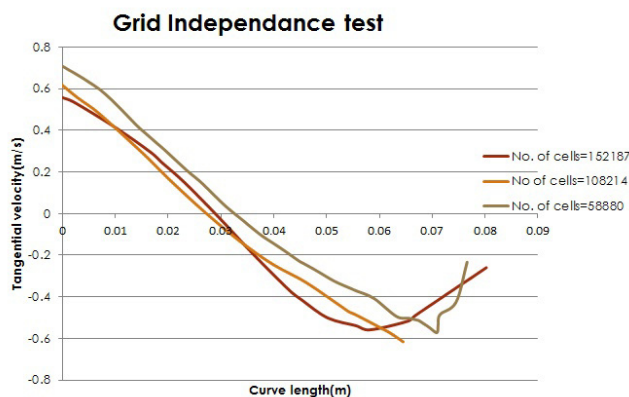


Fig. 3. Comparison of tangential velocity along line joining the center of circulation to the center of the mill for different mesh size.

## 5. Numerical Results and Discussion

### 5.1. Validation

The tangential velocity plot along a line passing through the center of the mill and the center of mass of the mill extended to the mill liners was compared with the PEPT experiment<sup>17,18,19</sup> to validate the model. Since the axial center of mass profile is not constant an average value of the center of mass is considered for the averaged solution for all three models. It is found out from the comparison that the pure DEM model overpredicts the tangential velocity as there is no damping of contact forces that are there due to the presence of the slurry. The pure CFD modeling of the slurry without the effect of the solids is not able to predict the velocity correctly as the forces acting on the slurry by the solids is predominant in this case as in case of tumbling mills the solids are having a higher velocity as compared to the fluids. The coupled DEM-CFD model which accounts for the effects of solid on the fluid gives a better comparison .

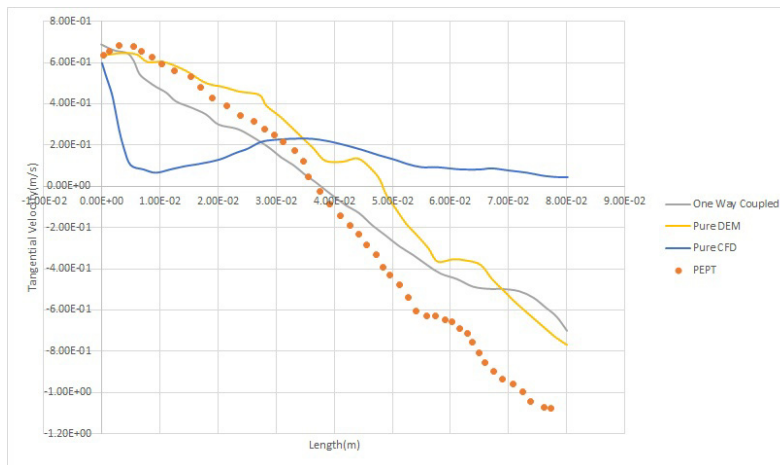


Fig. 4. Comparison of tangential velocity along line joining the center of circulation to the center of the mill with PEPT experimental results.

### 5.2. Pure DEM Model

The data obtained from the DEM simulations are processed using matlab subroutines to find out the axially averaged and time averaged solution. The solidicity contour and the free surface profile of the charge obtained from the spatial and temporal averaged solution was compared with equivalent PEPT results<sup>17,18,19</sup>.

#### 5.2.1. Solidicity Comparison

Figure 5 shows the qualitative comparison between the results obtained for dry DEM with the experimental data<sup>17</sup>. It can be observed from the figure that there is good agreement in the comparison except for the free surface region, since the pure DEM accounts for no damping due to the slurry motion a more random free surface profile was expected caused due to increased cataracting particles.

### 5.3. DEM-CFD coupled model

The fluid field data obtained from the coupled simulation were processed to find out the axial and time averaged solution and the transverse volume fraction was compared to the slurry profile obtained from the PEPT experimental results using smaller size particle tracer (i.e. size less than 1mm diameter)

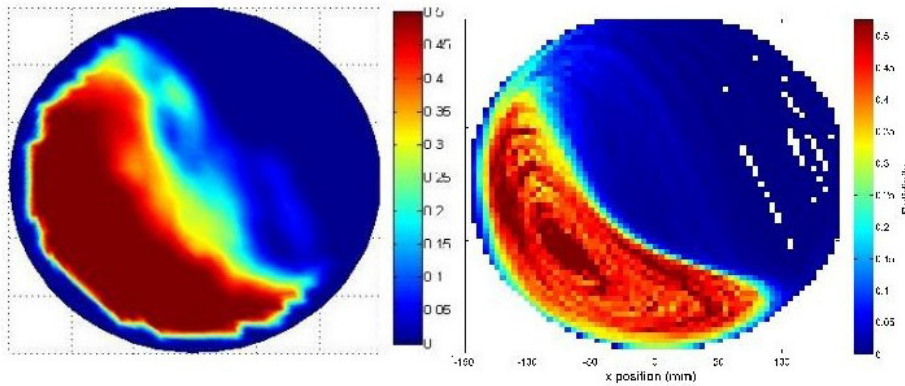


Fig. 5. Solidicity comparison between a)pure DEM model for 31.25 % loading and 60% critical speed of the mill and b)Equivalent PEPT result

5.3.1. Transverse Volume fraction

The free surface profile obtained from the time averaged and space averaged solution is compared with the equivalent profile obtained from PEPT experiments. Figure 8 and 9 shows the comparison of free surface profiles at different slurry concentration and rotational speed of the mill. Figure 6 and 7 shows the axially-averaged and time-averaged flow quantities for slurry only with 30% solids concentration by mass and no coupling in the 30 cm mill rotating at 75%  $v_{crit}$ . In the transverse direction, the bulk of the slurry remains almost stationary in the mill, with some slurry being dragged around the shell in a thin layer by the lifters. In a similar manner, small amounts of air are dragged under the slurry layer by the lifters on the right-hand side. These features of the slurry position and velocity profile hold over all of the 6 simulations. As observed from the quantified results the shoulder position of the the slurry reaches maximum height for the slurry concentration having 20% slurry as the velocity profile from the DEM is same for the different slurry concentration at 60% of the critical speed of the mill the effect of drag is maximum for the lowest density. With increased slurry density the drag force is reduced and consequently the height of the slurry shoulder position is reduced. With increased speed of rotation the shoulder position is increased slightly, major difference is at the toe region of the mill with increased speed the toe position is moved to the direction of mill rotation more than at lower speed. The coupled model is able to predict the slurry free surface profile the major difference between the numerical results and the experimentally found values are in the central region of the slurry where there is an absence of reduced slurry concentration. The difference arises from the fact that while very small size particles which were tracked for the slurry concentration in the PEPT experimental method it is modelled as bulk fluid with varying density in the proposed model.

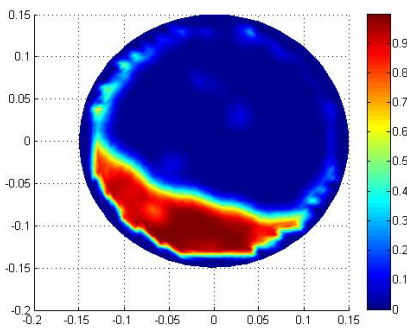


Fig. 6. Average transverse slurry fraction contour from pure CFD model at 30% solid concentration and 75% critical speed

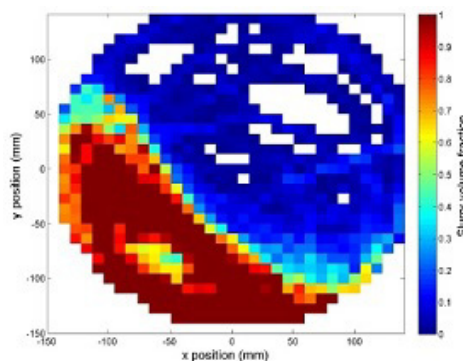


Fig. 7. PEPT Experimental result for 30% solid concentration 75% critical speed



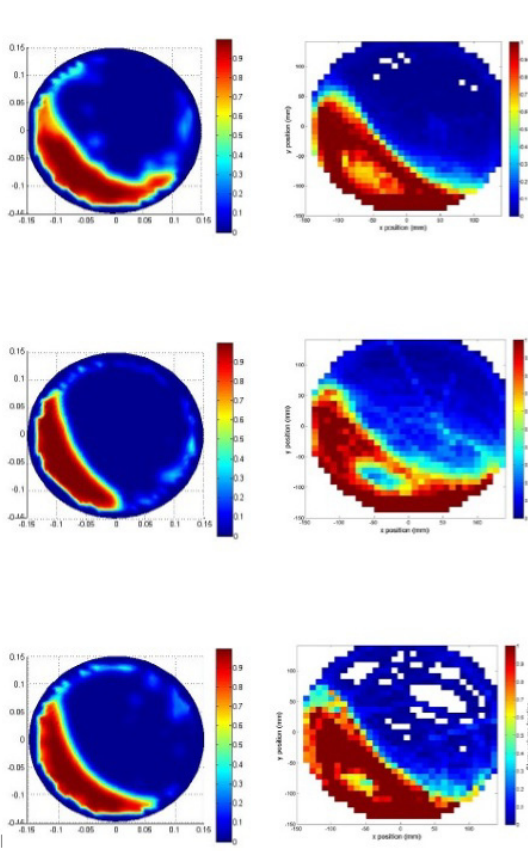


Fig. 8. Axially averaged and time averaged transverse volume fraction contour for top to bottom left: 20% solids and 60% critical speed, 20% solids and 75% critical speed and 30% solids and 60% critical speed right: equivalent PEPT results.

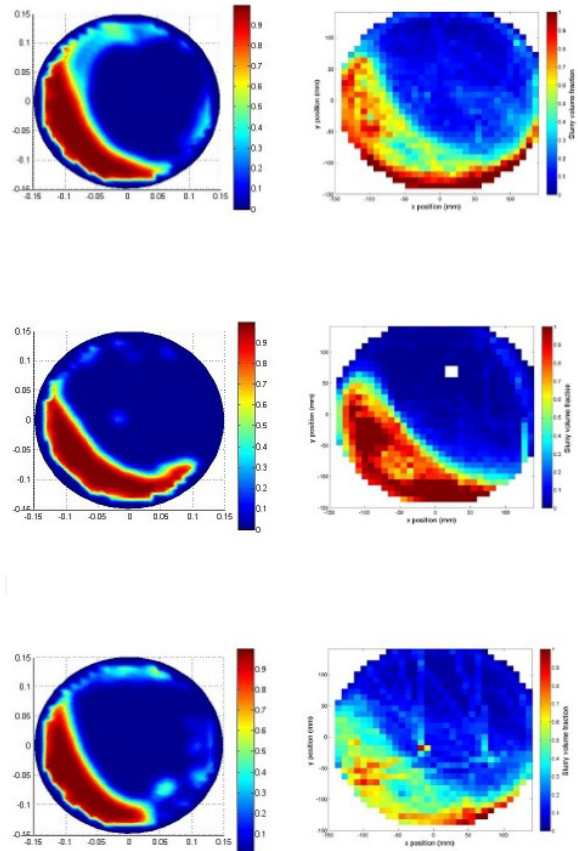


Fig. 9. Axially averaged and time averaged transverse volume fraction contour for top to bottom left: 30% solids and 75% critical speed, 40% solids and 60% critical speed and 40% solids and 75% critical speed right: equivalent PEPT results.

### 5.3.2. Axial center of mass profile

The velocity vector profile is shown in figure 10, the axial center of profile of the mill is calculated by locating the center of circulation along different axial length. The center of mass profile can be used to calculate the net power draw using the traditional torque arm approach. Figure 11 shows the comparison of axial center of mass profile for different mill rotation speed. The comparison shows the increase in the height of the center of mass at higher rotational velocities.

### 5.3.3. Effect of different drag models

The different multi-particle drag models are used to calculate the non-dimensional force term based on different solid concentration and Reynolds number. A comparison between the different drag models is shown in figure 12. It can be inferred that at higher particle Reynolds number the Ergun - wen yu drag computes a higher value than the Beeststra model. The effect of drag on the coupled model is examined figure 13. shows the comparison of the tangential velocity magnitude contour for the Ergun-Wen Yu and Beeststra drag and from the results in can be seen that in the Ergun drag case the velocity magnitude is higher at the slurry air interface due to higher particle Reynolds number in that region caused due to cascading particles.

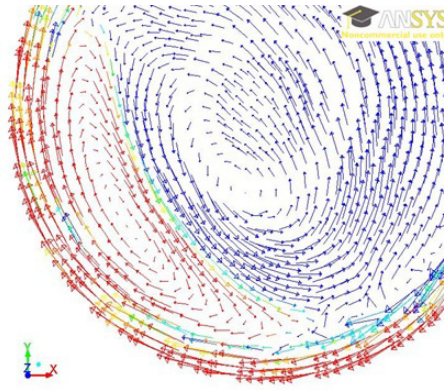


Fig. 10. Velocity vector plot of the slurry inside the mill from the coupled DEM-CFD model

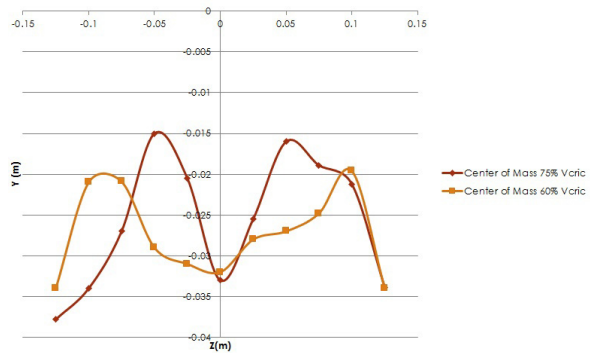


Fig. 11. Axial center of mass profile from the DEM-CFD coupled model

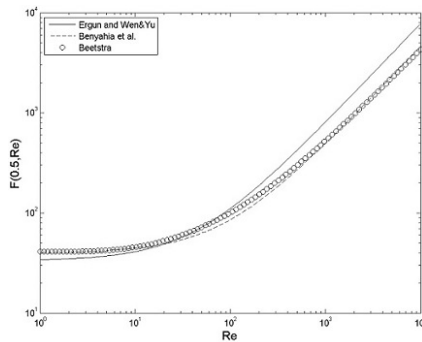


Fig. 12. Non dimensional drag force calculated for 0.5 solidicity using Ergun-Wen-yu , Beetstra drag models<sup>19</sup>

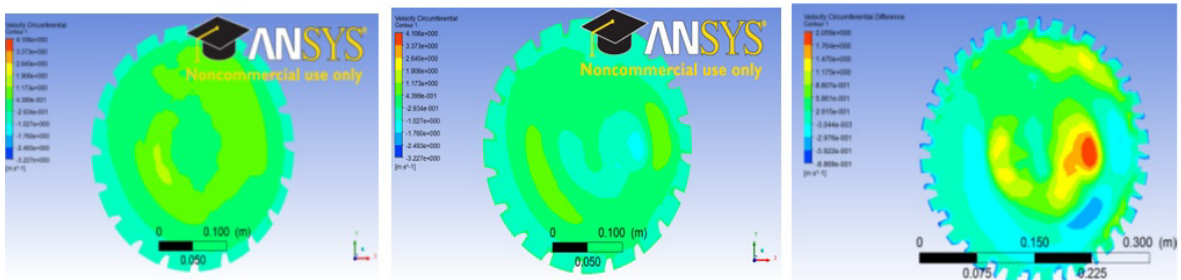


Fig. 13. Comparison of tangential velocity magnitude for different drag models from left to right Beeststra drag , Ergun Wen-yu drag difference between calculated values

**6. Conclusion**

The complex three phase flow can be modelled efficiently using coupled DEM-CFD model. The pure DEM model can effectively predict the particle flow but it generally over predicts as the effect of shear forces from the slurry is not accounted for. The pure CFD model fails to predict the free surface profile of the slurry air system inside the mill but the coupled model can effectively predict the free surface, so we infer that there is a major effect of drag forces of particle on the fluid. Once the drag force from the DEM simulation is incorporated as momentum source terms in the fluid cells the slurry profile from the coupled model gives a better comparison with the equivalent PEPT

experimental results. Future work is focussed on preparing a two way coupled model to account for the effect of slurry on solids and see the effect of different slurry concentration on the charge dynamics and vice-versa.

## References

1. K Schoenert. On the limitation of energy saving in milling. *Comminution* 1986.;
2. Lowrison, G.C. The size reduction of solid material. *Crushing and Grinding* 1974. 49-66; Macmillan; 1979.
3. EL-Shall, H., P. Somasundaran. Physico-Chemical Aspects of Grinding: a Review of Use of Additives. *Powder Technology* 1984.**38** 275-293;
4. Mishra, B.K. Rajamani, Raj K. The discrete element method for the simulation of ball mills. *Applied Mathematical Modelling* 1992.**16** 598-604;
5. Cleary, Paul W., A. Axial transport in dry ball mills. *Applied Mathematical Modelling* 2006.**30** 1343–1355;
6. Rajamani, R.K. Mishra, B.K. Venugopal, R. Datta, A. Discrete element analysis of tumbling mills. *Powder Technology* 2000.**108** 116-121;
7. Rajamani, Raj K. and Songfack, Poly and Mishra, B.K, A. Impact energy spectra of tumbling mills *Powder Technology* 2000.**109** 105–112;
8. D. Alkac. Modeling flow in the pulp lifter assembly using computational fluid Dynamics *Ph.D. Thesis , University of Utah* 2005.
9. Y. Tsuji, T. Kawaguchi, and T. Tanaka. Discrete particle simulation of two-dimensional Fluidized bed. *Powder Technology* 1993.**77** 79-87;
10. S. Yang, K. Luo, M. Fang, K. Zhang, and J. Fan. Parallel CFD-DEM modeling of the hydrodynamics in a lab-scale double slot-rectangular spouted bed with a partition plate. *Chemical Engineering Journal* 2014.**236** 158-170;
11. A. Amritkar, S. Deb, and D. Tafti. Efficient parallel CFD-DEM simulations using OpenMP. *Journal of Computational Physics* 2014.**256** 501-519;
12. P. W. Cleary, M. Sinnott, and R. Morrison. Prediction of slurry transport in SAG mills using SPH fluid flow in a dynamic DEM based porous media. *Minerals Engineering* 2006.**19** 1517-1527;
13. P. W. Cleary and R. Morrison. Understanding fine ore breakage in a laboratory scale ball mill using DEM. *Minerals Engineering* 2010.**24** 352-366;
14. Jayasundara, C.T. and Yang, R.Y. and Guo, B.Y. and Yu, A.B. and Rubenstein, J. Effect of slurry properties on particle motion in IsaMills. *Minerals Engineering* 2009.**22** 886-892;
15. Jayasundara, C.T. and Yang, R.Y. and Yu, A.B. Effect of slurry properties on particle motion in IsaMills. *Minerals Engineering* 2012.**33** 66-71;
16. Beetstra, Reneke. Drag force in random arrays of mono- and bidisperse spheres. *Ph.D. Thesis, University of Twente* 2006.;
17. I. Govender, N. Mangesana, A. Mainza, and J.-P. Franzidis. Measurement of shear rates in a laboratory tumbling mill. *Minerals Engineering* 2011.**24** 225-229;
18. L. Bbosa, I. Govender, A. Mainza, and M. Powell. Power draw estimations in experimental tumbling mills using PEPT *Minerals Engineering* 2011.**24** 319-324;
19. Malahe M., One way coupled dem-cfd model to simulate the free surface profile of slurry in a tumbling mill *M.S. Thesis University of Cape town* 2011.;
20. B. C. Blakey and D. F. James. Characterizing the rheology of laterite slurries. *International Journal of Minerals Processing* 2003.**70** 23-29;